

Three-terminal delta-doped barrier switching device with S-shaped negative differential resistance

J. N. Baillargeon, K. Y. Cheng, J. Laskar, and J. Kolodzey

Center for Compound Semiconductor Microelectronics and Coordinated Science Laboratory, University of Illinois at Urbana-Champaign, 1406 West Green Street, Urbana, Illinois 61801

(Received 14 April 1989; accepted for publication 6 June 1989)

A molecular beam epitaxial grown GaAs three-terminal device with a delta-doped barrier and GaInAs quantum well exhibiting controllable S-shaped negative differential resistance and switching voltages has been fabricated and tested. The device has a large potential barrier between the anode and cathode regions which can be modulated via a third terminal. The modulation of the potential barrier has a substantial effect on the switching behavior of the device. For the devices having a cathode contact area of $50 \mu\text{m}^2$, a spectrum analyzer reveals unstable oscillation up to the system measurement limit of 21 GHz. The output power signal for the best device is greater than -10 dBm which is 20 dB above the noise floor at 20.8 GHz. The results show this device to be a potentially useful and promising high-frequency oscillator.

Over the last two decades a variety of devices has displayed either N-shaped or S-shaped negative differential resistance (NDR). Devices possessing NDR have long been sought after as high-speed switches and as high-frequency oscillators because of their potential for power generation in the microwave and millimeter wave region. All of the S-shaped NDR devices having high-speed potential including the metal-insulator-semiconductor,¹ *p-n* junction,² superlattice,^{3,4} and heterojunction^{5,6} devices are two-terminal devices, and few have demonstrated microwave oscillation.^{4,7} While there are some S-shaped three-terminal devices having a NDR region, specifically triacs, there are no three-terminal S-shaped NDR devices capable of microwave frequency oscillation. In this letter, we report a new three-terminal delta-doped barrier switching device with controllable S-shaped NDR. Stable operation regions within the NDR region were also observed. The operation principle of the devices and their high-frequency performance are discussed.

The structures were grown in a Perkin-Elmer 430P molecular beam epitaxy system at a substrate temperature of 580 °C. The basic device structure, as shown in Fig. 1, consisted of a $1 \mu\text{m}$ Si-doped GaAs ($n = 3 \times 10^{18} \text{ cm}^{-3}$) buffer layer, followed by a 3000 Å undoped GaAs ($2 \times 10^{14} \text{ cm}^{-3}$), 100 Å Be-doped GaAs ($p = 8 \times 10^{18} \text{ cm}^{-3}$), 20 Å undoped GaAs spacer layer, 150 Å undoped $\text{Ga}_{1-x}\text{In}_x\text{As}$ ($x < 0.2$) quantum well, 20 Å undoped GaAs spacer layer, 100 Å Be-doped GaAs ($p = 8 \times 10^{18} \text{ cm}^{-3}$), 3000 Å undoped GaAs, and a 3000 Å Si-doped GaAs ($n = 3 \times 10^{18} \text{ cm}^{-3}$) cap layer.

After growth, $55 \mu\text{m} \times 100 \mu\text{m}$ mesas were patterned on the surface of the wafer using conventional photolithography and a wet chemical etch. Ohmic contacts having $50 \mu\text{m}^2$ areas were then formed to the cathode and anode regions by deposition of 350 Å Ge/150 Å Ni/1200 Å Au on the top and bottom n^+ layers, respectively, and alloyed at 400 °C for 15 s. The cap layer was then removed and photolithographically patterned grooves were then etched through the p^+ layers and into the bottom undoped GaAs layer using a wet chemical etch (1 H_2SO_4 :8 H_2O_2 :200 H_2O , 0 °C). Nonalloyed ohmic contacts of 350 Å Cr and 1200 Å Au were then deposited over these grooves to facilitate the gate contact. After pro-

cessing, the current-voltage (*I-V*) characteristics for the devices were measured using both a Tektronix 370 programmable curve tracer and a HP 4145A semiconductor parameter analyzer. Microwave oscillation spectra were observed using a Cascade Microtech probe, Tektronix 2755P spectrum analyzer, and a Tektronix 177 curve tracer that served as the bias supply.

The switching behavior of a typical device having three terminals is shown in Fig. 2 for three different bias conditions. It shows S-shaped *I-V* characteristics with a NDR region between the initial off-state voltage and the on-state voltage V_O . The application of either a positive or negative bias voltage at the third terminal controls the switching voltage across the cathode and anode regions. This bias voltage V_{GC} , measured relative to the cathode, raises and lowers the barrier height formed by the depleted *p* regions and quantum well as shown in Fig. 3(a). The GaInAs quantum well was included to enhance the localized confinement of the holes, particularly under bias. Since the devices were constructed symmetrically about the quantum well, the *I-V* characteristics were symmetric with bias. We note that switching has been observed in similar structures that do not contain a GaInAs quantum well, but the initial switching voltage was

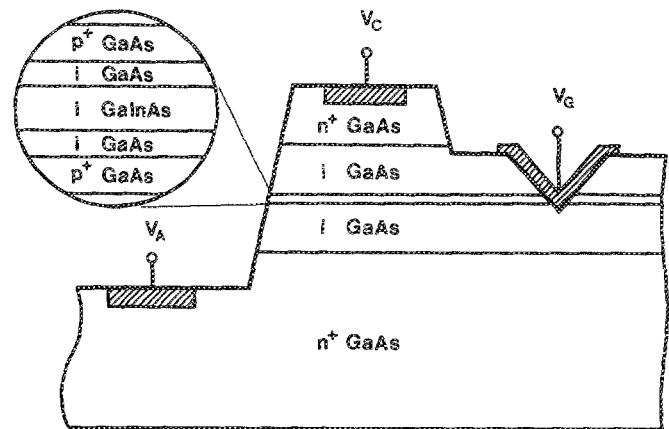


FIG. 1. Schematic cross section of the three-terminal delta-doped barrier S-shaped NDR device. V_C , V_A , and V_G are the cathode, anode, and gate voltages, respectively.

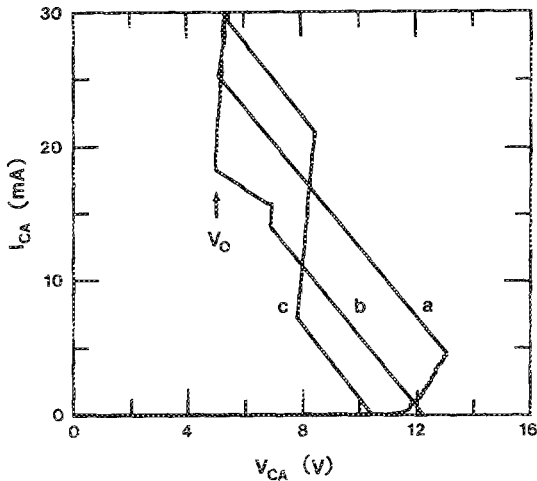


FIG. 2. Measured cathode to anode current-voltage characteristics ($I_{CA} - V_{CA}$) for three different gate to cathode bias voltage V_{GC} : (a) -2 V, (b) 2 V, and (c) 6 V. Notice the operating voltage of the stable region, which is characterized by a positive resistance, increases with increasing V_{GC} . The on-state voltage V_O is about 5 V.

lower and the on-state voltage V_O higher. The voltage V_{CA} for onset of NDR can then be varied by application of a suitable bias voltage V_{GC} . Typical switch back voltage for zero gate bias voltage V_{GC} were between 9 and 14 V. It is important to note that the third terminal is not acting as a hole injector, but as a bias route to vary the barrier height. Gate bias dependence gives a family of NDR curves and load lines, though the final on-state voltage appears to be independent of the bias. These devices also exhibited multiple

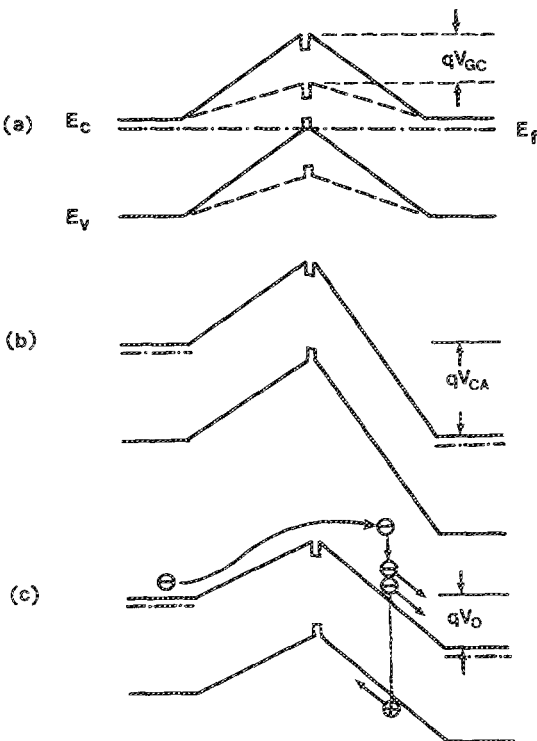


FIG. 3. Schematic of the energy-band structure for (a) gate bias voltage $V_{GC} = 0$ V (solid line) and $V_{GC} > 0$ V (dashed line) with cathode to anode voltage $V_{CA} = 0$ V, (b) off-state cathode to anode voltage V_{CA} with $V_{GC} = 0$ V just prior to switching, (c) on-state cathode to anode voltage V_O just after switching.

bias dependent stable operating regions characterized by the positive $I-V$ slope between the initial switching voltage and the final on-state voltage V_O within the NDR region. The operating voltage V_{CA} of the stable region increases as the bias voltage V_{GC} becomes increasingly positive. Reproducible $I-V$ characteristics exhibiting as many as four separate stable operating regions have been observed in some devices under a constant gate bias.

The switching mechanism responsible for NDR in these devices is attributed primarily to impact ionization. With the application of a cathode to anode voltage V_{CA} , the injected electrons from the cathode region cannot be thermionically emitted over the large energy barrier formed by the heavily doped p^+ regions as shown in Fig. 3(b). With increasing V_{CA} , relatively few carriers are able to tunnel through the energy barrier due to its thickness. As the applied voltage V_{CA} increases further, the injected electrons gain enough energy to overcome the barrier and initiate impact ionization in the intrinsic layer nearest the anode end. The process of impact ionization creates holes which become trapped in the valence band of the quantum well. As the holes accumulate in the quantum well, the energy barrier is lowered and the electron flow rapidly increases as they are now easily emitted over the lower barrier, hence, the onset of NDR [Fig. 3(c)]. At some bias voltage V_{GC} , the hole accumulation in the valence band along with the applied electric field between cathode and anode regions lowers the barrier to a point where the holes spill out of the well toward the cathode. This process of emptying the holes from the well raises the energy barrier and drives the device into a positive resistance stable operating region as seen in curves (b) and (c) of Fig. 2. As the applied voltage increases further, the process of impact ionization is reinitiated, hence, the onset of the second NDR region. The presence of impact ionization has been confirmed by the observation of infrared light emission in the NDR region. Since there are no holes injected by the third terminal, the light emission from the electron-hole recombination can only be attributed to holes created through impact ionization. A similar effect has been observed by Schubert,³ in heavily doped $n-p-n-p$ superlattices.

The oscillation spectrum of a typical device under zero gate bias conditions is displayed in Fig. 4. For the devices

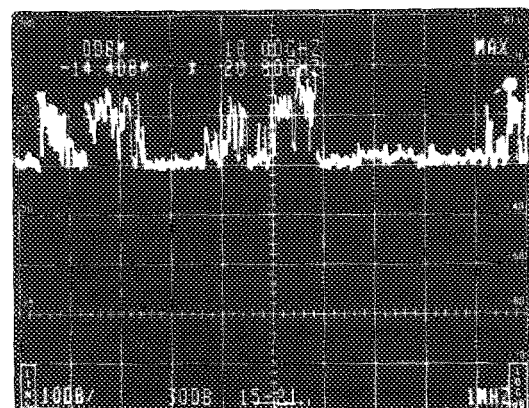


FIG. 4. Typical free-running microwave oscillation spectrum of a device operating in the NDR region between 15 and 21 GHz. Vertical scale is -10 dBm/div (top line = 0 dBm); horizontal scale is 600 MHz/div. The output power signal is 15.5 dB above the noise floor at 20.8 GHz.

tested without the aid of a resonant cavity, the spectrum analyzer indicates microwave oscillation with output power up to 21 GHz, the limit of the measurement system. This particular device, at 20.8 GHz, had an output power of -14.4 dBm which is 15.5 dB above the noise floor. The best measured device at 20.8 GHz had an output power of -9.6 dBm which was 20.4 dB above the noise floor. The effect of bias voltage on the microwave performance is under investigation and will be published elsewhere.

The maximum frequency of oscillation of this device is essentially determined by the speed in which the holes are swept out of the quantum well and across the intrinsic layer nearest the cathode. If, to first-order approximation, the on-state potential drop V_o across the device is distributed proportional to the layer thickness,⁸ then the hole velocity is conservatively 4×10^6 cm/s. Using a transit time calculation, the hole velocity limits the upper oscillation frequency to approximately 130 GHz for this particular device. By shortening the intrinsic layers, the maximum oscillation frequency should significantly increase and the onset of NDR will occur at a lower applied voltage.

In summary, we have fabricated and tested a three-terminal device exhibiting controllable S-shaped NDR. This

device was found to oscillate at microwave frequencies with significant output power and signal to noise ratio. Approximate theoretical calculations show this device to be potentially useful as an oscillator beyond 100 GHz.

We gratefully acknowledge K. Hess, the Hoosier brothers T. K. Higman and J. M. Higman, and G. E. Stillman for technical discussions. This work was supported by the National Science Foundation (CDR-22666) and the Research Board of the University of Illinois and equipment donations from Tektronix and Cascade Microtech.

¹T. Yamamoto and M. Morimoto, *Appl. Phys. Lett.* **20**, 269 (1972).

²C. E. C. Wood, I. F. Eastman, K. Board, K. Singer, and R. Malik, *Electron. Lett.* **18**, 676 (1982).

³E. F. Schubert, J. E. Cunningham, and W. T. Tsang, *Appl. Phys. Lett.* **51**, 817 (1987).

⁴A. M. Belyantsev, A. A. Ignatov, V. I. Piskarev, M. A. Sinitsyn, V. I. Shashkin, B. S. Yavich, and M. L. Yakovlev, *JETP Lett.* **43**, 437 (1986).

⁵K. Hess, T. K. Higman, M. A. Emanuel, and J. J. Coleman, *J. Appl. Phys.* **60**, 3775 (1986).

⁶G. W. Taylor, J. G. Simmons, A. Y. Cho, and R. S. Mand, *J. Appl. Phys.* **59**, 596 (1986).

⁷J. Kolodzey, J. Laskar, T. K. Higman, M. A. Emanuel, J. J. Coleman, and K. Hess, *IEEE Electron Device Lett.* **9**, 272 (1988).

⁸R. F. Kazarinov and S. Luryi, *Appl. Phys. Lett.* **38**, 810 (1981).